

Controls on the onset and termination of past hypoxia in the Baltic Sea

Nina M. Papadomanolaki^{a,*}, Nikki Dijkstra^a, Niels A.G.M. van Helmond^a, Mathilde Hagens^{a,1}, Thorsten Bauersachs^b, Ulrich Kotthoff^c, Francesca Sangiorgi^d, Caroline P. Slomp^a

^a Department of Earth Sciences, Geochemistry, Utrecht University, PO Box 80021, 3508 TA, Utrecht, The Netherlands

^b Institute of Geosciences, Department of Organic Geochemistry, Christian-Albrechts-University, Ludewig-Meyn-Str. 10, 24118 Kiel, Germany

^c Institute for Geology, Center of Natural History, Hamburg University, Bundesstr. 55, D-20146 Hamburg, Germany

^d Department of Earth Sciences, Marine Palynology and Paleoceanography, Utrecht University, PO Box 80115, 3508 TC Utrecht, The Netherlands



ARTICLE INFO

Keywords:

Holocene
Temperature
Salinity
Stratification
Productivity
Recovery

ABSTRACT

The Baltic Sea is currently the largest marine hypoxic ($O_2 < 2 \text{ mg L}^{-1}$) 'dead zone' following excessive nutrient input from anthropogenic activities over the past century. Widespread hypoxia has previously developed in the Baltic Sea during the Holocene Thermal Maximum (HTM; 8–4 ka before present; BP) and the Medieval Climate Anomaly (MCA; 1.4–0.7 ka BP). Here we study the mechanisms that contributed to the onset and termination of this past hypoxia using geochemical and marine palynological data from a sediment record retrieved from the Landsort Deep during IODP Expedition 347 (Site M0063). Dinoflagellate cyst records and TEX_{86}^L -based sea surface temperature reconstructions indicate a major increase in salinity and temperature prior to and across the onset of the HTM hypoxic interval, underlining the importance of both temperature and salinity stratification in providing conditions conducive to the onset of hypoxia. Both salinity and temperature decline during the termination of the HTM hypoxic interval. In contrast, we find no evidence for significant changes in surface salinity during the MCA hypoxic interval and both the onset and termination of hypoxia appear to have been primarily driven by changes in temperature. Our results indicate that temperature and salinity changes were key drivers of past hypoxia in the Baltic Sea and imply that ongoing climate change will delay recovery from the modern, nutrient-driven hypoxic event in the Baltic Sea.

1. Introduction

Hypoxia, i.e. dissolved oxygen concentrations in seawater $< 2 \text{ mg L}^{-1}$ (e.g. Rabalais et al., 2010), has been a recurring natural phenomenon in marine environments throughout Earth's history (e.g. Jenkyns, 2010). In the past decades, anthropogenic activities and global climate change have led to widespread hypoxia in coastal waters with harmful consequences for marine life (Diaz and Rosenberg, 2008).

The modern Baltic Sea is a key example of such a human-induced dead-zone (e.g. Conley et al., 2009; Carstensen et al., 2014a). Current efforts to mitigate the effects of hypoxia focus on reducing nutrient inputs from agriculture and sewage (Andersen et al., 2017). In addition, elevated temperatures contribute to the spread of hypoxia in multiple ways, e.g. by reducing the solubility of oxygen and stimulating marine productivity. Seawater temperatures are expected to increase further in the Baltic Sea region over the coming decades (BACC II Author Team, 2015), and may partly counteract the positive impact of nutrient

reduction. As a consequence, the timeline of recovery from hypoxia in the Baltic Sea remains uncertain (Meier et al., 2012).

Past intervals of hypoxia, recorded in marine sedimentary archives, provide the opportunity to study the various factors that control the development of hypoxia. In the Baltic Sea, two distinct intervals of widespread hypoxia are recognized prior to the modern hypoxic period (Zillén et al., 2008). Both intervals occurred in the ca. 8 ka following the transition from the freshwater Ancyclus lake phase to the brackish-marine Littorina phase (A/L transition, e.g. Björck, 1995). The first hypoxic interval was dated at 8–4 ka before present (BP) and coincided with the warm, dry period of the Holocene Thermal Maximum (HTM; e.g. Anderson et al., 1988; Zillén et al., 2008; Jilbert and Slomp, 2013). Diatom assemblages and the isotopic composition of organic matter from laminated sediments in the Gotland Basin record maxima in salinity, suggesting that the influx of saline North Sea waters after the A/L transition caused the expansion of hypoxia through water-column stratification (Emeis et al., 2003; Zillén et al., 2008). Hypoxia resulted in enhanced recycling of sedimentary phosphorus (P) and increased

* Corresponding author.

E-mail address: n.papadomanolaki@uu.nl (N.M. Papadomanolaki).

¹ Present address: Department of Soil Quality, Wageningen University & Research, Wageningen, the Netherlands.

marine productivity, thereby acting as a positive feedback on de-oxygenation (Sohlenius et al., 2001; Jilbert and Slomp, 2013). The termination of the HTM hypoxic interval (HTM_{HI}) has been attributed to reduced salinity and weakened stratification (Zillén et al., 2008; Carstensen et al., 2014a), and to the shoaling of the northern Åland Sea sill (Jilbert et al., 2015). This shoaling is thought to have led to re-oxygenation of the Bothnian Sea and, consequently, to an increase in the burial of P imported from the Baltic Proper. The associated decline in P availability in the Baltic Proper may have contributed to a decline in marine productivity and subsequent oxygen demand in deeper waters (Jilbert et al., 2015).

A large fraction of the Baltic Proper became hypoxic again between 1.4 and 0.7 ka BP, during the Medieval Climate Anomaly (MCA), when mean air temperatures were 0.9–1.4 °C higher than temperatures recorded in the period 1961–1990 (e.g. Mann et al., 2009; Jilbert and Slomp, 2013). Population estimates indicate that around the onset of the MCA hypoxic interval (MCA_{HI}) the human population in the Baltic Sea watershed expanded significantly and the associated release of nutrients from agriculture may have enhanced marine productivity (Zillén et al., 2008; Zillén and Conley, 2010). Kabel et al. (2012) proposed that a decrease in sea surface temperature (SST) at the end of the MCA_{HI} reduced marine productivity in the Baltic Sea and resulted in the termination of the hypoxic interval. A decrease in external nutrient loading due to a large population decline following the outbreak of the Black Death may have contributed to the termination as well (Zillén et al., 2008).

Various studies have focused on understanding environmental changes in the Baltic Sea region and their impact on the development of hypoxia during the HTM_{HI} and the MCA_{HI} using sediment records (e.g. Sohlenius et al., 2001; Zillén et al., 2008; Zillén and Conley, 2010) or climate modeling (Schimanke et al., 2012). However, major uncertainties remain regarding temporal changes in surface and bottom water salinity (Gustafsson and Westman, 2002; Emeis et al., 2003) and marine productivity (e.g. Brenner, 2005). Furthermore, currently only three SST records exist for the Baltic Sea. Two of these records are from the Baltic Proper, covering the past 1000 yr, excluding the HTM_{HI} and the early MCA_{HI} (Kabel et al., 2012), while the third is a low resolution record from an estuary in the Bothnian Sea (Warnock et al., 2017). Differences in sampling resolution and dating uncertainties further complicate comparison of the available records.

During Integrated Ocean Drilling Program (IODP) Expedition 347 a suite of long sediment cores was recovered from the Baltic Sea (Andrén et al., 2015a). Here, we present a high-resolution, multi-proxy study of sediments from the Landsort Deep (Site M0063, Fig. 1), capturing profiles of the onset and termination of the HTM_{HI} and MCA_{HI}. The combination of geochemical, lipid and palynological data allows the simultaneous reconstruction of variations in salinity and SST. We find that hypoxia during the HTM shows a strong link with changes in both salinity and temperature, while MCA hypoxia appears to have responded mainly to temperature changes.

2. Materials and methods

2.1. Study site and sample selection

For the past ~8 ka the Baltic Sea has been a restricted marginal sea that is strongly influenced by river runoff and saline inflows from the North Sea (Bergström and Carlsson, 1994; Gustafsson and Westman, 2002; Zillén et al., 2008). The deepest basin of the Baltic Sea is the Landsort Deep (459 m), which currently has a density stratified water column and bottom waters that are permanently euxinic (no oxygen and presence of free sulfide) (e.g. Zillén et al., 2008). The studied sediment record was retrieved from the central part of the Landsort Deep at Site M0063 (58°37.34'N, 18°15.25'E; 437 m water depth; Fig. 1) during IODP Expedition 347 in October 2013 (Andrén et al., 2015a).

The HTM_{HI} and MCA_{HI} were previously identified at this site based

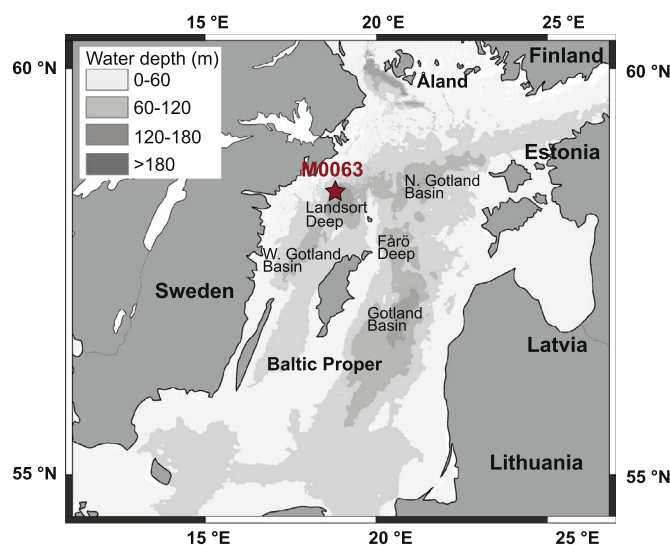


Fig. 1. Bathymetric map of the Baltic Proper. Site M0063 (red star) of IODP Expedition 347 is located in the Landsort Deep at a water depth of 437 m. (For interpretation of the references to color in this figure legend, the reader is referred to the web version of this article.)

on sedimentary enrichments in organic carbon (C_{org}), sulfur (S) and molybdenum (Mo) contents in ~9 m and ~4 m laminated intervals respectively (Dijkstra et al., 2016). Here, we focus on a selection of samples around the onset and termination of the HTM_{HI} and MCA_{HI}. These include 12 subsamples (~20 cm resolution; Hole C) previously studied by Dijkstra et al. (2016) and additional subsamples taken at 5 cm depth resolution from the sediments from Hole C at the IODP Core Repository in Bremen. While Andrén et al. (2015b) and Dijkstra et al. (2016) provided meters below seafloor (mbsf) depths, we use the new adjusted meters below seafloor (ambsf) depth scale. The difference in the two depth scales is caused by gas expansion of sediments during their recovery, which resulted in apparent depth overlap between consecutive sections (Obrochta et al., 2017). The ambfs depth scale eliminates this overlap. The chosen intervals cover the changes in C_{org} and Mo at the onset and termination of the HTM_{HI} and MCA_{HI} (Dijkstra et al., 2016): 27–24 ambfs, 21–17 ambfs, 7.2–6.3 ambfs and 3.9–3.3 ambfs. We also present geochemical data for 58 subsamples published by Dijkstra et al. (2016): 27–24 ambfs, 21–17 ambfs, 7.2–6.3 ambfs and 3.9–3.3 ambfs. TEX₈₆^L-based SSTs were determined for a total of 54 subsamples.

2.2. Sediment geochemistry

Sediment samples were freeze-dried and powdered with an agate mortar and pestle. Between 100 and 125 mg of sample was weighed in Teflon destruction vessels, after which 2.5 ml concentrated mixed acid ($HClO_4:HNO_3$; 3:2) and 2.5 ml 40% HF were added. The mixture was then heated to 90 °C and left overnight. Subsequently, the acids were evaporated at a temperature of 140 °C, after which the residue was dissolved in 25 ml 4.5% HNO_3 . Finally, the concentrations of iron (Fe), molybdenum (Mo) and aluminum (Al) were measured using Inductively Coupled Plasma-Optical Emission Spectrometry (ICP-OES) using a Perkin Elmer 9224 Optima 3000. Sedimentary Mo and Fe contents were normalized over Al. The relative standard deviation for the elements presented in this study was < 5% based on duplicate analysis.

Approximately 300 mg of powdered freeze-dried sediment was weighed in centrifuge tubes for decalcification prior to organic carbon analysis. The samples were mixed twice with 7.5 ml of 1 M HCl, shaken overnight and subsequently washed twice with 10 ml demineralized water (Van Santvoort et al., 2002). Afterwards, the samples were dried in an oven at 50 °C. Between 5 and 10 mg of decalcified sediment was

weighed in tinfoil cups and analyzed using a Fisons Instruments CNS NA 1500 analyzer. Sedimentary C_{org} content was calculated after correcting the sediment weight for carbonate loss. Duplicate analyses indicated that the relative standard deviation for C_{org} was < 5%.

A total of 54 sediment samples were freeze-dried, homogenized and extracted using a modified Bligh and Dyer technique (Rütters et al., 2002) at the Christian-Albrechts University. Up to 10 g of sediment was extracted ultrasonically for 10 min with a solvent mixture of methanol (MeOH): dichloromethane (DCM): phosphate buffer (2:1:0.8, v/v/v). The extract and residue were separated by centrifuging at 1500 rpm for 5 min, after which the supernatant was decanted into a new vial. This procedure was repeated until the extract was colorless. Subsequently, DCM and phosphate buffer were added to the combined extract to a volume ratio of 1:1:0.9 (v/v/v), which resulted in a phase separation. After centrifugation (2500 rpm, 5 min), the lipid-containing bottom layer was collected and the aqueous phase was washed twice with DCM. Subsequently, the combined DCM phases were reduced under rotary vacuum and transferred to glass vials, in which elemental sulfur was removed for 24 h by the addition of activated copper turnings. The obtained Bligh and Dyer extracts (BDEs) were then evaporated to dryness under a stream of nitrogen and stored at -20°C until further processing.

All BDEs were separated into apolar and polar lipid fractions using activated Al_2O_3 as stationary phase and hexane:DCM (9:1, v/v) and DCM:MeOH (1:1, v/v) as respective eluents. The polar fractions, containing glycerol dialkyl glycerol tetraethers (GDGTs), were dried under N_2 , re-dissolved in a mixture of hexane:propan-2-ol (99:1, v/v) to a concentration of 2 mg ml^{-1} and filtered through a $0.45\text{ }\mu\text{m}$ PTFE filter prior to analysis.

GDGTs were separated using a Waters Alliance 2695 high performance liquid chromatography (HPLC) system equipped with a Prevail Cyano column ($150\text{ mm} \times 2.1\text{ mm i.d.}$, $3\text{ }\mu\text{m}$; Grace, Deerfield, IL, USA) and following the analytical protocol described by Hopmans et al. (2000) and the gradient profile of Liu et al. (2012). Detection of isoprenoid and branched GDGTs was achieved using a Micromass ZQ single quadrupole mass spectrometer (MS) equipped with an APCI source operated in positive ion mode. MS conditions were as detailed in Heyng et al. (2015). All GDGTs were detected via single ion recording (SIR) of their protonated molecules (dwell time 234 ms) as described by Schouten et al. (2007).

TEX_{86}^L values were calculated following the formula of Kim et al. (2010) and transferred to SSTs using the Baltic Sea calibration of Kabel et al. (2012).

To determine the robustness of the TEX_{86}^L , we calculated the Branched and Isoprenoid Tetraether (BIT) index according to Hopmans et al. (2004). Empirical studies indicate that in settings where the BIT index exceeds the threshold of 0.3 (Weijers et al., 2006) or shows a correlation with TEX_{86}^L or its derivatives (Schouten et al., 2013) the reconstruction of SSTs using the distribution of isoprenoid GDGTs may be inaccurate.

2.3. Palynology

An aliquot of the freeze-dried sediment sample was gently crushed using an agate pestle and mortar. Subsequently, between 0.2 and 6.5 g of sediment was spiked with *Lycopodium clavatum* spores for quantification of palynomorph abundance (Wood et al., 1996). Samples were treated with HCl (10%) and HF (38%) to dissolve carbonates and silicates, respectively. The samples were centrifuged for 5 min at 2200 rpm and decanted to remove the acids. The samples were subsequently sieved over a $10\text{-}\mu\text{m}$ sieve and placed in an ultrasonic bath for 5 min to aid disaggregation of organic matter and remove minerals (e.g. pyrite). The retrieved residues were mounted on slides with glycerin gel and analyzed under a light microscope at a $400\times$ magnification. Identification was performed to genus and species level following Rochon et al. (1999), Fensome and Williams (2004) and Marret et al. (2004).

Averages of 189 (Maximum: 352; Minimum: 45, pre-A/L transition) and 118 (Maximum: 199; Minimum: 75) dinoflagellate cysts (dinocysts) were counted for the HTM and MCA, respectively. These averages are lower than the value of 300 counts usually considered sufficient to generate reliable diversities (e.g. Mertens et al., 2009). However, due to the low dinocyst diversity of Baltic Sea samples (Willumsen et al., 2013; Ning et al., 2015; Sildever et al., 2015), we are confident that these counts are representative of the sample content.

2.4. Proxy interpretation

2.4.1. Geochemical proxies

Changes in the sedimentary Fe and Mo contents can provide insight into past bottom water redox conditions (e.g. Helz et al., 1996; Lyons and Severmann, 2006; Scott and Lyons, 2012). In surface sediments on oxic shelves, Fe is generally present in the form of Fe-oxides. When oxygen concentrations decrease, Fe may be mobilized and transported to adjacent deep basins as nanoparticle Fe-oxides or complexed Fe(III) (Raiswell and Canfield, 2012). Increased Fe contents relative to a detrital background in deep basin sediments can therefore be used as an indicator of hypoxic conditions on the surrounding shelf (Lyons and Severmann, 2006; Raiswell and Canfield, 2012). The fraction of reactive Fe that is present as pyrite (FeS_2) (degree of pyritization; Raiswell et al., 1988) can be used to distinguish between sediments deposited under anoxic (> 0.38) and euxinic (0.7) bottom waters (Poulton and Canfield, 2011). Sediment Mo content can also be used to track past bottom water redox conditions (Scott and Lyons, 2012).

2.4.2. Palynological proxies

About 15 to 20% of extant dinoflagellates produce a fossilizable organic-walled dinocyst (e.g. Head, 1996). The distribution of dinoflagellates and their dinocysts is sensitive to a variety of environmental parameters, such as SST, salinity and marine productivity (Zonneveld et al., 2013), so that the presence and abundance of dinocyst species in down-core sediments can be employed to reconstruct paleoenvironmental conditions (e.g. de Vernal and Marret, 2007).

The process length of *Operculodinium centrocarpum* cysts in the Baltic Sea has been related to surface water salinity and is therefore applied as a (paleo-)salinity proxy (e.g. Mertens et al., 2011; Willumsen et al., 2013; Jansson et al., 2014; Ning et al., 2015). Here, we define an *O. centrocarpum* index, which we use as a qualitative indicator of salinity changes. The index is based on the relative abundance of morphotypes with processes over cysts without processes and is calculated as:

$$O. \text{ centrocarpum index} = \frac{\text{processes}}{\text{processes} + \text{no processes}} \quad (1)$$

We also used the cysts of *Gonyaulax apiculata* as an indicator for freshwater conditions. This species is a freshwater dinoflagellate (Evvitt et al., 1985) and its cyst has been found in lake sediments (e.g. Kouli et al., 2001).

2.5. Age model

For Site M0063, an age model was created for Hole D using the bulk ^{14}C method (Obrochta et al., 2017). We could not transfer this model to Hole C (this study), because of the large and variable depth offset between holes. Furthermore, an offset of on average $0.9 \pm 0.75\text{ ka}$ is observed for the onset and termination of the HTM_{HI} and MCA_{HI} when compared to earlier work (Jilbert and Slomp, 2013; Funkey et al., 2014; Lenz et al., 2015). These studies used an age model for Gotland Basin sediments developed using three different geochronological methods (Lougheed et al., 2012). Given the relative proximity of the Gotland Basin to the Landsort Deep, we expect the timing of the onset and termination of the hypoxic intervals to have been similar and we therefore use the ages of Lougheed et al. (2012).

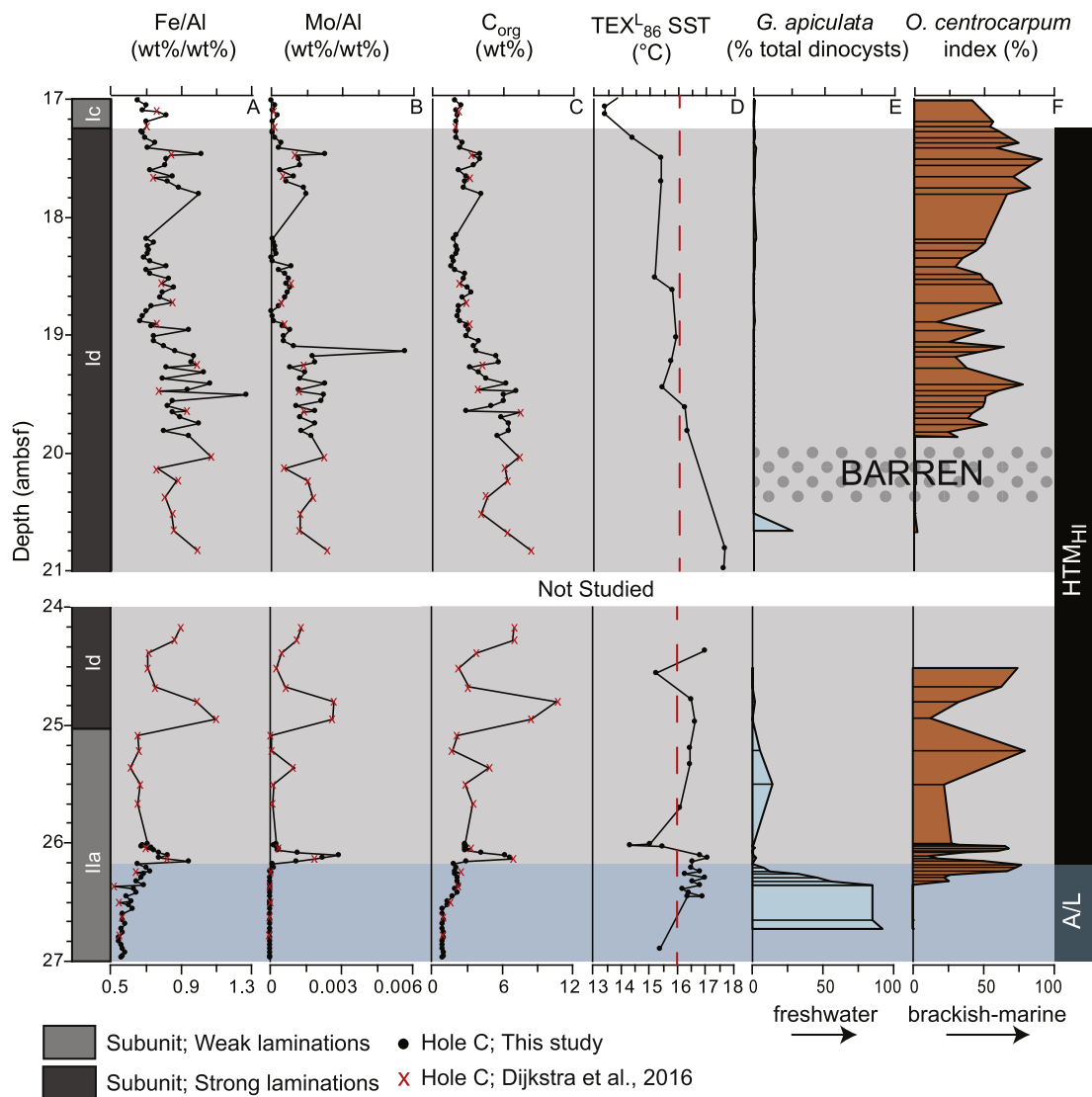


Fig. 2. Overview of geochemical and palynological data from Hole C, Site M0063 of the Landsort Deep for the depth intervals 27–24 ambsf and 21–17 ambsf. The onset (~26.2 ambsf) and termination (~17.2 ambsf) of the Holocene Thermal Maximum hypoxic interval (HTM_{HI}) are dated at approximately 8 ka and 4 ka BP, respectively. A. Iron over aluminum ratio (Fe/Al) B. Molybdenum over aluminum ratio (Mo/Al) C. Total organic carbon content (C_{org}) D. TEX₈₆^L sea surface temperatures E. Relative abundance of freshwater *Gonyaulax apiculata* cysts F. *Operculodinium centrocarpum* surface water salinity index. The dotted interval indicates barren samples that were devoid of palynomorphs. Red symbols in panels A–C represent data from Dijkstra et al. (2016) Units (Ic–Ila) represent the core lithology (Andrén et al., 2015b). A/L: Anclylus/Littorina transition (Dijkstra et al., 2016). (For interpretation of the references to color in this figure legend, the reader is referred to the web version of this article.)

3. Results

3.1. Anclylus/Littorina transition and the Holocene Thermal Maximum

The sediments deposited in the lower part of the A/L transition (27–26.6 ambsf) are low in Fe/Al (~0.6 wt%/wt%) and C_{org} (< 1 wt%), and depleted in Mo (2A–C). In the upper part (26.6–26.2 ambsf), Fe/Al increases (0.7 wt%/wt%) and the C_{org} content doubles (2 wt%), while Mo remains absent. Reconstructed SST increases from 15.4 °C to ~17 °C (Fig. 2D). Cysts of *G. apiculata* initially dominate the dinocyst assemblage (> 80%; Fig. 2E) but then decrease strongly (< 5%; above 26.4 ambsf).

At the onset of the HTM_{HI} (~26.2 ambsf), a distinct maximum in Fe/Al (> 0.9 wt%/wt%), Mo/Al and C_{org} (> 6 wt%) is observed. Sea surface temperatures are generally above 16 °C but decrease intermittently to 14.3 °C. A second maximum in Fe/Al, Mo/Al and C_{org} occurs between 25 and 24.7 ambsf. The *O. centrocarpum* index displays marked minima (< 0.1) during peak values of Fe/Al and Mo/Al (Fig. 2F).

The termination of the HTM_{HI} (~19.5–17.2 ambsf) is reflected in a decline to relatively low values of Fe/Al, Mo/Al and C_{org} (~0.7 wt%/wt%, < 0.0003 wt%/wt% and ~2 wt%, respectively). Prior to the termination, SST is 17.6 °C and during the termination a decline in SST to < 14 °C is observed. *G. apiculata* is mostly absent and there is no clear trend in the *O. centrocarpum* index.

3.2. The Medieval Climate Anomaly

Sediments deposited between 7.2 and 6.5 ambsf are relatively poor in Fe/Al (0.7 wt%/wt%), Mo/Al and C_{org} (1.5 wt%), and record SSTs around 14.7 °C (Fig. 3A–D). A few cysts of *G. apiculata* are infrequently present (Fig. 3E; H). The *O. centrocarpum* index (Fig. 3F) varies between 0.3 and 0.4.

Across the onset of the MCA_{HI} (6.5–6.3 ambsf), increases in Fe/Al (> 1 wt%/wt%), Mo/Al and C_{org} (> 2 wt%) are observed. Sea surface temperatures rise from ~14.6 °C to 16.5 °C. *G. apiculata* cysts disappear from the record. The C_{org} maximum (~5 wt%) is preceded by two maxima in the *O. centrocarpum* index (~0.7).

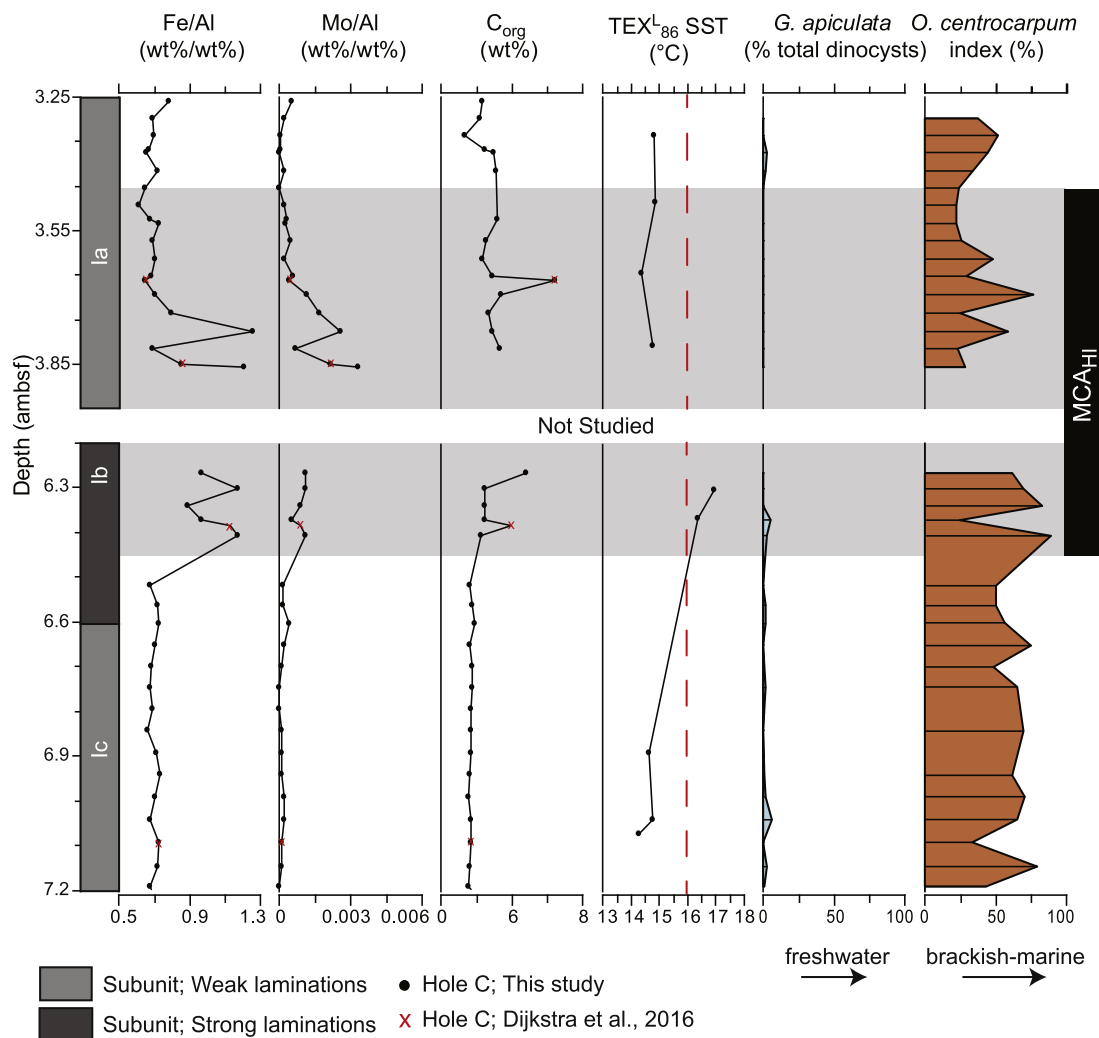


Fig. 3. Overview of geochemical and palynological data from Hole C, Site M0063 of the Landsort Deep for the intervals of 7.2–6.3 ambsf and 3.9–3.3 ambsf. The onset (~6.5 ambsf) and termination (~3.5 ambsf) of the Medieval Climate Anomaly hypoxic interval (MCA_{HI}) are dated at approximately 1.4 ka and 0.7 ka BP, respectively. A. Iron over aluminum ratio (Fe/Al) B. Molybdenum over aluminum ratio (Mo/Al) C. Total organic carbon content (C_{org}) D. TEX₈₆^L sea surface temperatures E. Relative abundance of freshwater *Gonyaulax apiculata* cysts F. *Operculodinium centrocarpum* surface water salinity index Red symbols in panels A–C indicate data from Dijkstra et al. (2016). Units (Ia–Ic) represent the core lithology (Andrén et al., 2015b). (For interpretation of the references to color in this figure legend, the reader is referred to the web version of this article.)

The termination of the MCA_{HI} (3.9–3.5 ambsf) is characterized by a general decrease in Fe/Al and Mo/Al. Values of C_{org} are relatively constant at ~2.9 wt%. Following the termination, values for Fe/Al and C_{org} are on average 0.7 wt%/wt% and 2 wt%, respectively. Mo is only intermittently present. TEX₈₆^L-reconstructed SSTs between 14 °C and 15 °C precede the termination. There is no clear trend in the *O. centrocarpum* index.

4. Discussion

4.1. Environmental conditions during the transition to the brackish-marine Littorina Sea

The onset of the brackish-marine Littorina Sea is recorded in Landsort Deep sediments by the gradual appearance of benthic foraminifera and brackish-marine diatoms in Unit IIB (Andrén et al., 2015b) and by a strong decline in the abundance of freshwater *G. apiculata* cysts (26.4–26.2 ambsf, Fig. 2E). This disappearance of *G. apiculata* was previously observed in the Gotland Basin, where it is dated at ca. 7.6–7.4 ka BP (Brenner, 2005). This date matches the timing of the rise in bottom water salinity at our site (ca. 7.5 ka BP; Egger et al., 2017).

The increase in Fe/Al during the A/L transition (Fig. 2A) likely reflects a decrease in oxygen concentrations on the shelf surrounding the Landsort Deep and an associated increase in the lateral transfer of Fe from the shelf and subsequent burial in the deep basin (“Fe shuttling”; Raiswell and Canfield, 2012; Lenz et al., 2015). The decrease in shelf bottom water oxygen was likely the result of decreased oxygen solubility and increased stratification due to the incursion of saline North Sea waters, in combination with increasing SSTs (Fig. 2D; Renssen et al., 2012; Kotthoff et al., 2017). The reconstruction of SSTs from TEX₈₆^L is validated by the BIT index (Supplements, Supp. Table 3) which is generally below 0.16 (Supp. Figs. 1, 2), with the exception of the sample at 26.89 ambsf which had a BIT value of 0.32. As SSTs increased they crossed the temperature threshold for cyanobacterial bloom formation of 16 °C (Fig. 2D; Wasmund, 1997). This, together with increased P availability (e.g. Bianchi et al., 2000; Sohlenius et al., 2001) likely stimulated an increase in cyanobacterial productivity, which contributed to bottom water deoxygenation upon degradation (Funkey et al., 2014).

4.2. Onset and termination of hypoxia during the Holocene Thermal Maximum

4.2.1. Onset of the HTM_{HI}

The onset of the HTM_{HI} (ca. 8 ka BP; Zillén et al., 2008; Jilbert and Slomp, 2013) is reflected in a continued increase in Fe/Al in the Landsort Deep, indicating an intensification of the Fe shuttle in response to widespread hypoxia in the Baltic Proper. In addition, elevated Mo/Al values (Fig. 2B) throughout the onset, combined with the high degree of pyritization (> 0.7, Dijkstra et al., 2016) indicates that bottom waters in the Landsort Deep were euxinic during the HTM_{HI} (Poulton and Canfield, 2011; Scott and Lyons, 2012).

The onset of the HTM_{HI} occurred after the establishment of brackish-marine conditions in the Baltic Proper and Landsort Deep, within an extended period characterized by high SSTs that started during the A/L transition. We therefore infer that the emplacement of a permanent halocline was the main cause for the development of widespread hypoxia, while temperature-driven stratification provided conditions conducive to hypoxia. In addition, maxima in C_{org}, Fe/Al and Mo/Al (26.2 ambsf; 25–24.7 ambsf) coincide with low *O. centrocarpum* index values, suggesting relatively low sea surface salinity (Fig. 2F). This trend would be opposite to the increasing trend in bottom water salinity (Gustafsson and Westman, 2002; Egger et al., 2017), leading to a larger density difference between surface and bottom waters, thus stimulating water-column stratification. Possible causes for lower surface water salinity are a high North Atlantic Oscillation (NAO) index and the retraction of Norwegian glaciers due to HTM warming (e.g. Hänninen et al., 2000; Nesje, 2009), which would both lead to enhanced freshwater input.

4.2.2. Termination of the HTM_{HI}

The termination of the HTM_{HI} in the Landsort Deep and the surrounding shelf area is reflected in a phased decrease in Fe/Al and Mo/Al (Fig. 2A,B). This suggests a muted Fe shuttle, due to retreating shelf hypoxia, and less reducing conditions in the bottom waters of the Landsort Deep, respectively, in agreement with previous studies (Funkey et al., 2014; Lenz et al., 2015; Dijkstra et al., 2016).

The absence of a correlation between the geochemical parameters and the *O. centrocarpum* index, and the lack of a clear trend in the *O. centrocarpum* index itself, suggest that sea surface salinity neither changed considerably nor contributed to the termination of the HTM_{HI} therefore surface water salinity. However, decreasing bottom water salinity during the termination, due to a weakened connection between the Baltic Sea and North Sea from ca. 5.5 ka BP onwards (Gustafsson and Westman, 2002; Egger et al., 2017), would have weakened stratification. The steady decline in SSTs further reduced stratification, increased oxygen solubility and likely caused a decrease in cyanobacterial productivity as SSTs dropped below 16 °C (Westman et al., 2003; Funkey et al., 2014).

4.3. Onset and termination of hypoxia during the Medieval Climate Anomaly

4.3.1. Onset of the MCA_{HI}

The onset of the MCA_{HI} in the Landsort Deep is characterized by an increase in Mo/Al, S and C_{org} at 6.45 ambsf (Dijkstra et al., 2016). The high values of Fe/Al and the intermittent presence of Mo (Fig. 3A–B) below this depth indicates that this site and its surrounding area were already experiencing low oxygen conditions prior to the MCA_{HI}. The increase in Mo/Al across the onset and the average degree of pyritization of 0.64 throughout the MCA_{HI} (Dijkstra et al., 2016) imply that bottom waters in the Landsort Deep were anoxic and possibly euxinic.

Model simulations indicate that the onset of the MCA_{HI} occurred within a long-term period of decreasing bottom water salinity (Gustafsson and Westman, 2002; Egger et al., 2017). The absence of a correlation between Fe/Al, Mo/Al and the *O. centrocarpum* index

suggests that stratification resulting from salinity differences was not important for the development of the MCA_{HI}. We infer that climatic warming, leading to lower gas solubility and promoting water column stratification, was the primary cause of the MCA_{HI}. The prevailing high SSTs (> 16 °C) coupled with the terrestrial input of P as a result of an expanding human population and associated marine productivity may have contributed to the development of hypoxia (e.g. Zillén et al., 2008; Zillén and Conley, 2010; Funkey et al., 2014).

4.3.2. Termination of the MCA_{HI}

A coeval decrease in Fe/Al and Mo/Al marks the retreat of shelf hypoxia in the Landsort Deep as well as the onset of less reducing conditions in the deep basin itself. Similar changes in both ratios were recorded in sediments from other sites in the Baltic Proper (Jilbert and Slomp, 2013; Funkey et al., 2014; Lenz et al., 2015) at the end of the MCA_{HI}.

Due to the continued decrease in bottom water salinity (Gustafsson and Westman, 2002; Egger et al., 2017) and the lack of a signal in the *O. centrocarpum* index we conclude that salinity changes did not contribute to the termination of the MCA_{HI}. Sea surface temperatures during the termination are significantly lower than during the onset (Fig. 3D), in line with lower air temperatures (e.g. Seppä et al., 2009), suggesting that the actual drop in SST preceded the termination of the MCA_{HI}. A large SST decrease, similar in shape to the decline we observe in our Fe/Al and Mo/Al records, was reported previously for the nearby Gotland Basin (Kabel et al., 2012), supporting the conclusion that a decline of SST at or near the end of the MCA_{HI} would have resulted in weakened water column stratification, facilitating bottom water ventilation. The SST decrease (< 16 °C) would also have reduced cyanobacterial productivity (Funkey et al., 2014).

4.4. Causes of hypoxia and consequences for the future Baltic Sea

In the modern Baltic Sea, widespread hypoxia is primarily linked to the high loading of nutrients through river discharge and the resulting enhanced marine productivity, with global warming playing a secondary role (Carstensen et al., 2014b). During the HTM_{HI} and MCA_{HI} we find that changes in salinity and SST were key causes of hypoxia, underscoring their possible importance in facilitating the spread of oxygen-depleted bottom waters in the future Baltic Sea. Model simulations indicate that the average salinity in the Baltic Sea will probably decrease over the coming century, presumably weakening stratification (Meier, 2006; Meier et al., 2011; BACC II Author Team, 2015). Yet, future changes in global and local sea level, as well as a different NAO mode, may result in opposite trends in surface and bottom water salinity. This could potentially lead to enhanced water column stratification and facilitate a further expansion of hypoxia in the Baltic Sea (Meier et al., 2016), as observed during the HTM_{HI}.

Our results highlight that changes in SST contributed to the onset and termination of both the HTM_{HI} and MCA_{HI}. Warming surface waters already contribute to bottom water de-oxygenation today (Conley et al., 2002) and the projected temperature rise for the Baltic Sea in the coming century (Meier et al., 2012; BACC II Author Team, 2015) is within or above the range of SST change for the HTM and MCA (~2 °C; this study; Kabel et al., 2012). Warmer future SSTs may therefore cause a further decline in oxygen concentrations through decreased oxygen solubility, enhanced stratification and by supporting cyanobacterial blooms.

Despite a reduction in external nutrient loads, the ecological status for large parts of the Baltic Sea is showing only gradual improvement (Andersen et al., 2017). This is mostly attributed to internal storage and recycling of P under hypoxic conditions (Andersen et al., 2017). Our findings are in agreement with previous studies (e.g. Andersson et al., 2015 and references therein), and indicate that mitigation schemes must also account for changes in salinity and temperature and their possible effect on Baltic Sea oxygen concentrations.

5. Conclusions

Our study highlights that changes in salinity and sea surface temperature (SST) were key drivers of past intervals of widespread hypoxia in the Baltic Sea. During the Holocene Thermal Maximum (HTM), the hypoxic interval followed the transition to a warmer and more saline Baltic Sea. The onset of HTM hypoxia coincided with a period of relatively fresh surface waters, suggesting that enhanced stratification due to the larger salinity difference between surface and bottom water played a key role. During the Medieval Climate Anomaly the onset of widespread hypoxia correlated with changes in SST. Both onsets likely coincided with enhanced marine productivity, because the critical SST ($> 16\text{ }^{\circ}\text{C}$) for the development of cyanobacterial blooms was reached. We infer that both terminations were mainly caused by decreased stratification due to lower SSTs and, at the end of the HTM_{HT}, a weaker salinity gradient. Our findings underline the potential impact of ongoing global climate change on bottom water oxygen concentrations in the Baltic Sea. Importantly, they indicate that current efforts to address hypoxia by curbing nutrient input from land may be countered by rising temperatures and an increased gradient between surface and bottom water salinity, linked to sea level change. These results underscore the importance of understanding future climate dynamics when designing mitigation schemes for eutrophic systems.

Supplementary data to this article can be found online at <https://doi.org/10.1016/j.palaeo.2017.11.012>.

Acknowledgments

Samples used in this study were provided by the Integrated Ocean Drilling Program (IODP). We thank the captain, crew and scientists of IODP Expedition 347 for their contribution to the sample collection. We also thank Ton Zalm, Helen de Waard and Arnold van Dijk for analytical assistance at Utrecht University. This research was funded by ERC Starting Grant 278364 and NWO-Vici Grant 865.13.005 to C. P. Slomp. T. Bauersachs received financial support through DFG grant BA 3841/5-1 and BA 3841/5-2. This work was carried out under the program of the Netherlands Earth System Science Centre (NESSC), financially supported by the Ministry of Education, Culture and Science (OCW).

References

- Andersen, J.H., Carstensen, J., Conley, D.J., Dromph, K., Fleming-Lehtinen, V., Gustafsson, B.G., Josefson, A.B., Norkko, A., Villnäs, A., Murray, C., 2017. Long-term temporal and spatial trends in eutrophication status of the Baltic Sea. *Biol. Rev.* 92 (1), 135–149.
- Anderson, P.M., Barnosky, C.D., Bartlein, P.J., Behling, P.J., Brubaker, L., Cushing, E.J., Dodson, J., Dworetzky, B., Guetter, P.J., Harrison, S.P., Huntley, B., Kutzbach, J.E., Markgraf, V., Marvel, R., McGlone, M.S., Mix, A., Moar, N.T., Morley, J., Perrott, R.A., Peterson, G.M., Prell, W.L., Prentice, I.C., Ritchie, J.C., Roberts, N., Ruddiman, W.F., Salinger, M.J., Spaulding, W.G., Street-Perrott, F.A., Thompson, R.S., Wang, P.K., Webb III, T., Winkler, M.G., Wright Jr, H.E., 1988. Climatic changes of the last 18,000 years: observations and model simulations. *Science* 241, 1043–1052.
- Andersson, A., Meier, H.M., Ripszám, M., Rowe, O., Wikner, J., Haglund, P., Eilola, K., Legrand, C., Figueroa, D., Paczkowska, J., Lindehoff, E., Tysklind, A., Elmgren, R., 2015. Projected future climate change and Baltic Sea ecosystem management. *Ambio* 44 (3), 345–356.
- Andrén, T., Jørgensen, B.B., Cotterill, C., Green, S., Andrén, E., Ash, J., Bauersachs, T., Cragg, B., Fanget, A.S., Fehr, A., Granaszewski, W., Groeneveld, J., Hardisty, D., Herrero-Bervera, E., Hyttinen, O., Jensen, J.B., Johnson, S., Kenzler, M., Kotilainen, A., Kotthoff, U., Marshall, I.P.G., Martin, E., Obrochta, S., Passchier, S., Quintana Krupinski, N., Riedinger, N., Slomp, C., Snowball, I., Stepanova, A., Strano, S., Torti, A., Warnock, J., Xiao, N., Zhang, R., 2015a. Summary. In: Andrén, T., Jørgensen, B.B., Cotterill, C., Green, S., Expedition 347 Scientists (Eds.), Proc. IODP, 347: College Station, TX (Integrated Ocean Drilling Program).
- Andrén, T., Jørgensen, B.B., Cotterill, C., Green, S., Andrén, E., Ash, J., Bauersachs, T., Cragg, B., Fanget, A.S., Fehr, A., Granaszewski, W., Groeneveld, J., Hardisty, D., Herrero-Bervera, E., Hyttinen, O., Jensen, J.B., Johnson, S., Kenzler, M., Kotilainen, A., Kotthoff, U., Marshall, I.P.G., Martin, E., Obrochta, S., Passchier, S., Quintana Krupinski, N., Riedinger, N., Slomp, C., Snowball, I., Stepanova, A., Strano, S., Torti, A., Warnock, J., Xiao, N., Zhang, R., 2015b. Site M0063. In: Andrén, T., Jørgensen, B.B., Cotterill, C., Green, S., Expedition 347 Scientists (Eds.), Proc. IODP, 347: College Station, TX (Integrated Ocean Drilling Program).
- BACC II Author Team, 2015. Second Assessment of Climate Change for the Baltic Sea Basin. Springer International Publishing, AG Switzerland.
- Bergström, S., Carlsson, B., 1994. River runoff to the Baltic Sea – 1950–1990. *Ambio* 23 (4–5), 280–287.
- Bianchi, T.S., Engelhaupt, E., Westman, P., Andrén, T., Rolff, C., Elmgren, R., 2000. Cyanobacterial blooms in the Baltic Sea: natural or human-induced? *Limnol. Oceanogr.* 45 (3), 716–726.
- Björck, S., 1995. A review of the history of the Baltic Sea, 13.0–8.0 ka BP. *Quat. Int.* 27 (94), 19–40.
- Brenner, W.W., 2005. Holocene environmental history of the Gotland Basin (Baltic Sea)—a micropalaeontological model. *Palaeogeogr. Palaeoclimatol. Palaeoecol.* 220 (3), 227–241.
- Carstensen, J., Conley, D.J., Bonsdorff, E., Gustafsson, B.G., Hietanen, S., Janas, U., Jilbert, T., Maximov, A., Norkko, A., Norkko, J., Reed, D.C., Slomp, C.P., Timmermann, K., Voss, M., 2014a. Hypoxia in the Baltic Sea: biogeochemical cycles, benthic fauna, and management. *Ambio* 43, 26–36.
- Carstensen, J., Andersen, J.H., Gustafsson, B.G., Conley, D.J., 2014b. Deoxygenation of the Baltic Sea during the last century. *Proc. Natl. Acad. Sci.* 111 (15), 5628–5633.
- Conley, D.J., Humborg, C., Rahm, L., Savchuk, O.P., Wulff, F., 2002. Hypoxia in the Baltic Sea and basin-scale changes in phosphorus biogeochemistry. *Environ. Sci. Technol.* 36 (24), 5315–5320.
- Conley, D.J., Björck, S., Bonsdorff, E., Carstensen, J., Destouni, G., Gustafsson, B.G., Hietanen, S., Kortekaas, M., Kuosa, H., Meier, H.E.M., Müller-Karulis, B., Nordberg, K., Norkko, A., Nürnberg, G., Pitkänen, H., Rabalais, N.N., Rosenberg, R., Savchuk, O.P., Slomp, C.P., Voss, M., Wulff, F., Zillén, L., 2009. Hypoxia-related processes in the Baltic Sea. *Environ. Sci. Technol.* 43, 3412–3420.
- Diaz, R.J., Rosenberg, R., 2008. Spreading dead zones and consequences for marine ecosystems. *Science* 321 (5891), 926–929.
- Dijkstra, N., Slomp, C.P., Behrends, T., 347 scientists, Expedition, 2016. Vivianite is a key sink for phosphorus in sediments of the Landsort Deep, an intermittently anoxic deep basin in the Baltic Sea. *Chem. Geol.* 438, 58–72.
- Egger, M., Hagens, M., Sapart, C.J., Dijkstra, N., van Helmond, N.A.G.M., Mogollón, J.M., Risgaard-Petersen, N., van der Veen, C., Kasten, S., Riedinger, N., Böttcher, M.E., Röckmann, T., Jørgensen, B.B., Slomp, C.P., 2017. Iron oxide reduction in methane-rich deep Baltic Sea sediments. *Geochim. Cosmochim. Acta* 207, 256–276.
- Emeis, K.C., Struck, U., Blanz, T., Kohly, A., Voß, M., 2003. Salinity changes in the central Baltic Sea (NW Europe) over the last 10,000 years. *The Holocene* 13 (3), 411–421.
- Evitt, W.R., Gocht, H., Netzel, H., 1985. Gonyaulax cysts from lake Zürich sediments. *Rev. Palaeobot. Palynol.* 45 (1–2), 35–46.
- Fensome, R.A., Williams, G.L., 2004. The Lentin and Williams Index of Fossil Dinoflagellates, 2004 Edition. AASP Contrib. Ser., 42, Am. Assoc. of Stratigr. Palynol. Found., Dartmouth, Nova Scotia, Canada.
- Funkey, C.P., Conley, D.J., Reuss, N.S., Humborg, C., Jilbert, T., Slomp, C.P., 2014. Hypoxia sustains cyanobacteria blooms in the Baltic Sea. *Environ. Sci. Technol.* 48 (5), 2598–2602.
- Gustafsson, B.G., Westman, P., 2002. On the causes for salinity variations in the Baltic Sea during the last 8500 years. *Paleoceanography* 17 (3) (12–1).
- Hänninen, J., Vuorinen, I., Hjelt, P., 2000. Climatic factors in the Atlantic control the oceanographic and ecological changes in the Baltic Sea. *Limnol. Oceanogr.* 45 (3), 703–710.
- Head, M.J., 1996. Late Cenozoic dinoflagellates from the Royal Society borehole at Ludham, Norfolk, eastern England. *J. Paleontol.* 70 (04), 543–570.
- Helz, G.R., Miller, C.V., Charnock, J.M., Mosselmans, J.F.W., Patrick, R.A.D., Garner, C.D., Vaughan, D.J., 1996. Mechanism of molybdenum removal from the sea and its concentration in black shales: EXAFS evidence. *Geochim. Cosmochim. Acta* 60 (19), 3631–3642.
- Heyng, A.M., Mayr, C., Lücke, A., Moschen, R., Wissel, H., Striewski, B., Bauersachs, T., 2015. Middle and Late Holocene paleotemperatures reconstructed from oxygen isotopes and GDGTs of sediments from Lake Pupuke, New Zealand. *Quat. Int.* 374, 3–14.
- Hopmans, E.C., Schouten, S., Pancost, R.D., van der Meer, M.T.J., Sinnighe Damsté, J.S., 2000. Analysis of intact tetraether lipids in archaeal cell material and sediments by high performance liquid chromatography/atmospheric pressure chemical ionization mass spectrometry. *Rapid Commun. Mass Spectrom.* 14, 585–589.
- Hopmans, E.C., Weijers, J.W., Schefuß, E., Herfort, L., Damsté, J.S.S., Schouten, S., 2004. A novel proxy for terrestrial organic matter in sediments based on branched and isoprenoid tetraether lipids. *Earth Planet. Sci. Lett.* 224 (1), 107–116.
- Jansson, I.M., Mertens, K.N., Head, M.J., de Vernal, A., Londeix, L., Marret, F., Matthiessen, J., Sangiorgi, F., 2014. Statistically assessing the correlation between salinity and morphology in cysts produced by the dinoflagellate *Protoceratium reticulatum* from surface sediments of the North Atlantic Ocean, Mediterranean–Marmara–Black Sea region, and Baltic–Kattegat–Skagerrak estuarine system. *Palaeogeogr. Palaeoclimatol. Palaeoecol.* 399, 202–213.
- Jenkyns, H.C., 2010. Geochemistry of oceanic anoxic events. *Geochem. Geophys. Geosyst.* 11 (3), 1–30.
- Jilbert, T., Slomp, C.P., 2013. Rapid high-amplitude variability in Baltic Sea hypoxia during the Holocene. *Geology* 41 (11), 1183–1186.
- Jilbert, T., Conley, D.J., Gustafsson, B.G., Funkey, C.P., Slomp, C.P., 2015. Glacio-isostatic control on hypoxia in a high-latitude shelf basin. *Geology* 43 (5), 427–430.
- Kabel, K., Moros, M., Porsche, C., Neumann, T., Adolphi, F., Andersen, T.J., Siegel, H., Gerth, M., Leipe, T., Jansen, E., Sinnighe Damsté, J.S., 2012. Impact of climate change on the Baltic Sea ecosystem over the past 1,000 years. *Nat. Clim. Chang.* 2, 871–874.
- Kim, J.H., van der Meer, J., Schouten, S., Helmke, P., Willmott, V., Sangiorgi, F., Koc, N., Hopmans, E.C., Sinnighe Damsté, J.S., 2010. New indices and calibrations derived from the distribution of crenarchaeal isoprenoid tetraether lipids: implications for past sea surface temperature reconstructions. *Geochim. Cosmochim. Acta* 74, 4639–4654.

- Kotthoff, U., Groeneveld, J., Ash, J.L., Fanget, A.S., Quintana Krupinski, N., Peyron, O., Stepanova, A., Warnock, J., van Helmond, N.A.G.M., Passey, B.H., Clausen, O.R., Bennike, O., Andr n, E., Granoszewski, W., Andr n, T., Filipsson, H.L., Seidenkrantz, M., Slomp, C.P., Bauersachs, T., 2017. Reconstructing Holocene temperature and salinity variations in the western Baltic Sea region: A multi-proxy comparison from the Little Belt (IODP Expedition 347, Site M0059). In: Biogeosciences Discussions, (accepted for publication).
- Kouli, K., Brinkhuis, H., Dale, B., 2001. *Spiniferites cruciformis*: a fresh water dinoflagellate cyst? Rev. Palaeobot. Palynol. 113 (4), 273–286.
- Lenz, C., Jilbert, T., Conley, D.J., Slomp, C.P., 2015. Hypoxia-driven variations in iron and manganese shuttling in the Baltic Sea over the past 8 ka. Geochim. Geophys. Geosyst. 16 (10), 3754–3766.
- Liu, X.L., Summons, R.E., Hinrichs, K.U., 2012. Extending the known range of glycerol ether lipids in the environment: structural assignments based on tandem mass spectral fragmentation patterns. Rapid Commun. Mass Spectrom. 26, 2295–2302.
- Lougheed, B.C., Snowball, I., Moros, M., Kabel, K., Muscheler, R., Virtasalo, J.J., Wacker, L., 2012. Using an independent geochronology based on palaeomagnetic secular variation (PSV) and atmospheric Pb deposition to date Baltic Sea sediments and infer ¹⁴C reservoir age. Quat. Sci. Rev. 42, 43–58.
- Lyons, T.W., Severmann, S., 2006. A critical look at iron paleoredox proxies: new insights from modern euxinic marine basins. Geochim. Cosmochim. Acta 70 (23), 5698–5722.
- Mann, M.E., Zhang, Z., Rutherford, S., Bradley, R.S., Hughes, M.K., Shindell, D., Ammann, C., Falwieg, G., Ni, F., 2009. Global signatures and dynamical origins of the Little Ice Age and Medieval Climate Anomaly. Science 326, 1256–1260.
- Marret, F., Leroy, S., Chali , F., Fran oise, F., 2004. New organic-walled dinoflagellate cysts from recent sediments of Central Asian seas. Rev. Palaeobot. Palynol. 129 (1), 1–20.
- Meier, H.E.M., 2006. Baltic Sea climate in the late twenty-first century: a dynamical downscaling approach using two global models and two emission scenarios. Clim. Dyn. 27 (1), 39–68.
- Meier, H.E.M., Andersson, H.C., Eilola, K., Gustafsson, B.G., Kuznetsov, I., Mller-Karulis, B., Neumann, T., Savchuk, O.P., 2011. Hypoxia in future climates: a model ensemble study for the Baltic Sea. Geophys. Res. Lett. 38, 1–6.
- Meier, H.E.M., Andersson, H.C., Arheimer, B., Blenckner, T., Chubarenko, B., Donnelly, C., Eilola, K., Gustafsson, B.G., Hansson, A., Havenhand, J., H glund, A., Kuznetsov, I., MacKenzie, B.R., M ller-Karulis, B., Neumann, T., Niiranen, S., Piwowarczyk, J., Raudsepp, U., Reckermann, M., Ruoho-Airola, T., Savchuk, O.P., Schenk, F., Schimanke, S., V li, G., Weslawski, J.-M., Zorita, E., 2012. Comparing reconstructed past variations and future projections of the Baltic Sea ecosystem—first results from multi-model ensemble simulations. Environ. Res. Lett. 7, 34005.
- Meier, H.E.M., H glund, A., Eilola, K., Almr th-Rosell, E., 2016. Impact of accelerated future global mean sea level rise on hypoxia in the Baltic Sea. Clim. Dyn. 1–10.
- Mertens, K.N., Verhoeven, K., Verleye, T., Louwye, S., Amorim, A., Ribeiro, S., Deaf, A.S., Harding, I.C., De Schepper, S., Gonz lez, C., Kodrans-Nsiah, M., De Vernal, A., Henry, M., Radi, T., Dybkjaer, K., Poulsen, N.E., Feist-Burkhardt, S., Chitolie, J., Heilmann-Clausen, C., Londeix, L., Turon, J.-L., Marret, F., Matthiessen, J., McCarthy, F.M.G., Prasad, V., Pospelova, V., Kyffin Hughes, J.E., Riding, J.B., Rochon, A., Sangiorgi, F., Welters, N., Sinclair, N., Thun, C., Soliman, A., Van Nieuwenhove, N., Vink, A., Young, M., 2009. Determining the absolute abundance of dinoflagellate cysts in recent marine sediments: the Lycopodium marker-grain method put to the test. Rev. Palaeobot. Palynol. 157, 238–252.
- Mertens, K.N., Dale, B., Ellegaard, M., Jansson, I., Godhe, A., Kremp, A., Louwye, S., 2011. Process length variation in cysts of the dinoflagellate *Protoceratium reticulatum*, from surface sediments of the Baltic–Kattegat–Skagerrak estuarine system: a regional salinity proxy. Boreas 40 (2), 242–255.
- Nesje, A., 2009. Latest Pleistocene and Holocene alpine glacier fluctuations in Scandinavia. Quat. Sci. Rev. 28 (21), 2119–2136.
- Ning, W., Andersson, P.S., Ghosh, A., Khan, M., Filipsson, H.L., 2015. Quantitative salinity reconstructions of the Baltic Sea during the mid-Holocene. Boreas 46, 100–110.
- Obrochta, S.P., Andr n, T., Fazekas, S.Z., Lougheed, B.C., Snowball, I., Yokoyama, Y., Miyairi, Y., Kondo, R., Kotilainen, A.T., Hyttinen, O., Fehr, A., 2017. The undatables: quantifying uncertainty in a highly expanded Late Glacial–Holocene sediment sequence recovered from the deepest Baltic Sea basin—IODP Site M0063. Geochim. Geophys. Geosyst. 18 (3), 858–871.
- Poulton, S.W., Canfield, D.E., 2011. Ferruginous conditions: a dominant feature of the ocean through Earth's history. Elements 7 (2), 107–112.
- Rabalais, N.N., Diaz, R.J., Levin, L.A., Turner, R.E., Gilbert, D., Zhang, J., 2010. Dynamics and distribution of natural and human-caused hypoxia. Biogeosciences 7 (2), 585–619.
- Raiswell, R., Canfield, D.E., 2012. The iron biogeochemical cycle past and present. Geochim. Perspect. 1 (1), 1–2.
- Raiswell, R., Buckley, F., Berner, R.A., Anderson, T.F., 1988. Degree of pyritization of iron as a paleoenvironmental indicator of bottom-water oxygenation. J. Sediment. Res. 58 (5), 812–819.
- Renssen, H., Sepp , H., Crosta, X., Goosse, H., Roche, D.M., 2012. Global characterization of the Holocene thermal maximum. Quat. Sci. Rev. 48, 7–19.
- Rochon, A., Vernal, A.D., Turon, J.L., Matthieffen, J., Head, M.J., 1999. Distribution of Recent Dinoflagellate Cysts in Surface Sediments From the North Atlantic Ocean and Adjacent Seas in Relation to Sea-surface Parameters. American Association of Stratigraphic Palynologists Contribution Series 35. pp. 1–146.
- R tters, H., Sass, H., Cypionka, H., Rullk tter, J., 2002. Phospholipid analysis as a tool to study complex microbial communities in marine sediments. J. Microbiol. Methods 48, 149–160.
- Schimanke, S., Meier, H.E.M., Kjellstr m, E., Strandberg, G., Hordoir, R., 2012. The climate in the Baltic Sea region during the last millennium simulated with a regional climate model. Clim. Past 8 (5), 1419–1433.
- Schouten, S., Hugu t, C., Hopmans, E.C., Kienhuis, M.V.M., Sinninghe Damst , J.S., 2007. Analytical methodology for TEX86 paleothermometry by high-performance liquid chromatography/atmospheric pressure chemical ionization-mass spectrometry. Anal. Chem. 79, 2940–2944.
- Schouten, S., Hopmans, E.C., Rosell-Mel , A., Pearson, A., Adam, P., Bauersachs, T., Bard, E., Bernasconi, S.M., Bianchi, T.S., Brocks, J.J., Carlson, L.T., Derenne, S., Selver, A.D., Dutta, K., Eglinton, T., Fosse, C., Galy, V., Grice, K., Hinrichs, K.U., Huang, Y., Hugu t, A., Hugu t, C., Hurley, S., Ingalls, A., Jia, G., Keely, B., Knappy, C., Kondo, M., Krishnan, S., Lincoln, S., Lipps, J., Mangelsdorf, K., Mart nez-Garc a, A., M not, G., Mets, A., Mollenhauer, G., Ossebaar, J., Pagani, M., Pancost, R.D., Pearson, E.J., Peterse, F., Reichert, G.J., Schaeffer, P., Schmitt, G., Schwark, L., Shah, S.R., Smith, R.W., Smittenberg, R.H., Summons, R.E., Takano, Y., Talbot, H.M., Taylor, K.W.R., Tarozo, R., Uchida, M., van Dongen, B.E., Van Mooy, B.A.S., Wang, J., Warren, C., Weijers, J.W.H., Werne, J.P., Woltering, M., Xie, S., Yamamoto, M., Yang, H., Zhang, C.L., Zhang, Y., Zhao, M., Sinninghe Damst , J.S., 2013. An interlaboratory study of TEX86 and BIT analysis of sediments, extracts, and standard mixtures. Geochim. Geophys. Geosyst. 14, 1–23.
- Scott, C., Lyons, T.W., 2012. Contrasting molybdenum cycling and isotopic properties in euxinic versus non-euxinic sediments and sedimentary rocks: refining the paleo-proxies. Chem. Geol. 324, 19–27.
- Sepp , H., Bju ne, A.E., Telford, R.J., Birks, H.J.B., Veski, S., 2009. Last nine-thousand years of temperature variability in northern Europe. Clim. Past 5 (3), 523–535.
- Silvever, S., Andersen, T.J., Ribeiro, S., Ellegaard, M., 2015. Influence of surface water salinity gradient on dinoflagellate cyst community structure, abundance and morphology in the Baltic Sea, Kattegat and Skagerrak. Estuar. Coast. Shelf Sci. 155, 1–7.
- Sohlenius, G., Emeis, K.C., Andr n, E., Andr n, T., Kohly, A., 2001. Development of anoxia during the Holocene fresh–brackish water transition in the Baltic Sea. Mar. Geol. 177 (3), 221–242.
- Van Santvoort, P.J.M., De Lange, G.J., Thomson, J., Colley, S., Meysman, F.J.R., Slomp, C.P., 2002. Oxidation and origin of organic matter in surficial eastern Mediterranean hemipelagic sediments. Aquat. Geochem. 8 (3), 153–175.
- de Vernal, A., Marret, F., 2007. Organic-walled dinoflagellate cysts: tracers of sea-surface conditions. Dev. Marine Geol. 1, 371–408.
- Warnock, J.P., Bauersachs, T., Kotthoff, U., Brandt, H.T., Andr n, E., 2017. Holocene environmental history of the  ngerman lven Estuary, northern Baltic Sea. Boreas. <http://dx.doi.org/10.1111/bor.12281>.
- Wasmund, N., 1997. Occurrence of cyanobacterial blooms in the Baltic Sea in relation to environmental conditions. Int. Rev. Hydrobiol. Hydrogr. 82 (2), 169–184.
- Weijers, J.W., Schouten, S., Spaargaren, O.C., Sinninghe Damst , J.S., 2006. Occurrence and distribution of tetraether membrane lipids in soils: implications for the use of the TEX₈₆ proxy and the BIT index. Org. Geochem. 37 (12), 1680–1693.
- Westman, P., Borgendahl, J., Bianchi, T.S., Chen, N., 2003. Probable causes for cyanobacterial expansion in the Baltic Sea: role of anoxia and phosphorus retention. Estuaries 26 (3), 680–689.
- Willumsen, P.I., Filipsson, H.L., Reinholdsson, M., Lenz, C., 2013. Surface salinity and nutrient variations during the Littorina stage in the F r  deep, Baltic Sea. Boreas 42 (1), 210–223.
- Wood, G.D., Gabriel, A.M., Lawson, J.C., 1996. Palynological techniques—processing and microscopy. Palynol. Princ. Appl. 1, 29–50.
- Zill n, L., Conley, D.J., 2010. Hypoxia and cyanobacteria blooms—are they really natural features of the late Holocene history of the Baltic Sea? Biogeosciences 7 (8), 2567–2580.
- Zill n, L., Conley, D.J., Andr n, T., Andr n, E., Bj rck, S., 2008. Past occurrences of hypoxia in the Baltic Sea and the role of climate variability, environmental change and human impact. Earth Sci. Rev. 91 (1–4).
- Zonneveld, K.A.F., Marret, F., Versteegh, G.J.M., Bogus, K., Bonnet, S., Bouimetarhan, I., Crouch, E., de Vernal, A., Elshaniwan, R., Edwards, L., Esper, O., Forke, S., Grosfjeld, K., Henry, M., Holzwarth, U., Kiehl, J.F., Kim, S.Y., Ladouceur, S., Ledu, D., Chen, L., Limoges, A., Londeix, L., Lu, S.H., Mahmoud, M.S., Marino, G., Matsouka, K., Matthiessen, J., Mildenhall, D.C., Mudie, P., Neil, H.L., Pospelova, V., Qi, Y., Radi, T., Richerol, T., Rochon, A., Sangiorgi, F., Solignac, S., Turon, J.L., Verleye, T., Wang, Y., Wang, Z., Young, M., 2013. Atlas of modern dinoflagellate cyst distribution based on 2405 data points. Rev. Palaeobot. Palynol. 191, 1–197.